Earth and Planetary Science Letters 292 (2010) 39–50

Contents lists available at ScienceDirect

Earth and Planetary Science Letters

journal homepage: www.elsevier.com/locate/epsl

Andean uplift, ocean cooling and Atacama hyperaridity: A climate modeling perspective

René D. Garreaud [a,*], Alejandra Molina [a], Marcelo Farias [b]

[a] FCMF, Departamento de Geofísica, Universidad de Chile, Blanco Encalada 2002, Santiago, Chile
[b] FCFM, Departmento de Geología, Universidad de Chile, Plaza Ercilla 803, Santiago, Chile

ARTICLE INFO

Article history:
Received 13 May 2009
Received in revised form 28 December 2009
Accepted 8 January 2010
Available online 11 February 2010

Editor: M.L. Delaney

Keywords:
Atacama
aridity
Andean uplift
ocean cooling
climate model

ABSTRACT

Located along the west coast of subtropical South America, the Atacama Desert features an extremely dry climate in sharp contrast with relatively wet conditions over the Central Andes and farther east. The Atacama's hyperaridity has been attributed to its subtropical location, the cold waters over the adjacent southeast Pacific Ocean and the presence of the Andes Cordillera. Although geological evidence reveals less dry conditions in the remote past, the timing of the arid-to-hyperarid transition is a matter of controversy. Several studies suggest that such transition occurred between 19 and 13 Ma fostered by the concurrent uplift of the Andes during the lower–middle Miocene. Other studies, however, suggest a much earlier (~25 Ma) or later (2–1 Ma) transition associated with global or regional ocean cooling. Here we use PLASIM, a simple global climate model, to study the effect of the Andean surface uplift and sea surface temperature changes upon Atacama aridity. In one set of experiments, the continental topography was scaled by a factor ranging from 0.9 to 0.1. Decreasing the height of the Andes did not increase precipitation over the Atacama region, but rather decrease the precipitation over the Central Andes and the interior of the continent. These results, consistent with previous modeling studies, suggest that the Andean uplift was not an important ingredient in the onset of Atacama hyperaridity, even if both events overlapped in time. A globally uniform sea surface warming does not result in a significant increase of precipitation over the Atacama. In contrast, a regional warming over the subtropical southeast Pacific very effectively increase precipitation along the west coast of South America by decreasing the subsidence and the dry advection at low levels. It suggested that a reinforcement of the Humboldt Current since the late Miocene and particularly during the Pliocene/Pleistocene transition was crucial in the drying of the Atacama Desert that culminated with the present day hyperarid conditions.

1. Introduction

Arid conditions prevail along the west coast of South America all the way from the subtropics to near the equator. This long but narrow strip of land, bounded by the Pacific Ocean and the Andes Cordillera, includes the Atacama Desert in northern Chile and southern Perú (25–17 °S, Fig. 1), arguably the driest place on earth (Lettau, 1978). Mean annual precipitation (MAP) below 5 mm is not uncommon in stations along the coast and over the Preandean Central Depression (at about 1000 ma.s.l.); in practice, most of this amount is due to drizzle from coastal stratus and very unusual (once every 10 or more years) rainfall episodes associated with the passage of a cold front (Garreaud and Rutllant, 1996; Vargas et al., 2006). MAP increases over the western slope of the Andes reaching 100–200 mm at the height of the Western Cordillera, caused by "spill over" from convective storms that develop further east over the Central Andes Altiplano (Fig. 1). The Altiplano itself, about 4000 ma.s.l. mean elevation, receives 100–400 mm per year, largely concentrated during the austral summer when solar heating destabilizes the local troposphere and the establishment of upper-level easterly winds favors the transport of moist air from the interior of the continent (Garreaud et al., 2003; Vuille et al., 2003; Falvey and Garreaud, 2005). To the east of the Central Andes, rainfall is more evenly distributed (MAP ~200–500 mm) but still exhibits a well-defined maximum during austral summer in connection with the development of the so-called South American Monsoon (Zhou and Lau, 1998; Vera et al., 2006).

A primary cause for Atacama aridity is its location at the eastern boundary of the subtropical Pacific. In that region, large-scale atmospheric subsidence produces dry, stable conditions and maintains a surface anticyclone over the southeast Pacific (e.g., Rodwell and Hoskins, 2001) that hinders the arrival of mid-latitude disturbances. The subtropical anticyclone drives equatorward winds along the coast that, in turn, foster the transport of cold waters from higher latitudes (i.e., the Humbold or Chile–Perú surface current),

* Corresponding author. Department of Geophysics, Universidad de Chile, Blanco Enclada 2002, Santiago, Chile. Tel.: +56 2 9784310.
E-mail address: rgarreau@dgf.uchile.cl (R.D. Garreaud).

0012-821X/$ – see front matter © 2010 Elsevier B.V. All rights reserved.
doi:10.1016/j.epsl.2010.01.017

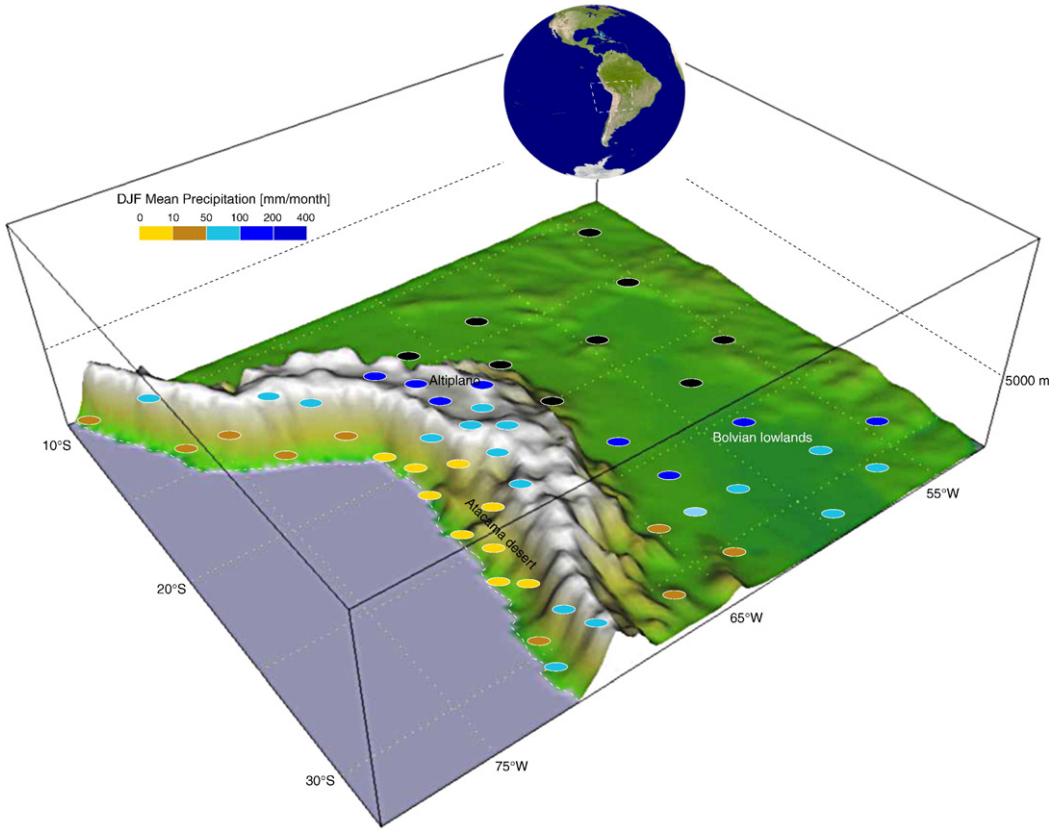

Fig. 1. Austral summer (DJF) long-term mean precipitation over subtropical South America (area indicated in inset) displayed over terrain elevation. The circles are placed over selected stations included in the Global Historical Climate Network (GHNC; Peterson and Vose, 1997) color coded according to the precipitation amount.

force upwelling of deep waters, and leads to the formation of a persistent deck of stratus clouds (Takahashi and Battisti, 2007). These factors result in a marked regional cooling of the lower troposphere that is compensated by enhanced subsidence along the Atacama coast (Wang et al., 2004; Takahashi and Battisti, 2007) further drying this area. The presence of the Andes Cordillera has been regarded as an additional factor for the dryness of the Atacama. The effect of the Andes on continental precipitation has been documented, among others, by Virji (1981), Lenters and Cook (1995) and more recently by Insel et al. (2009). This formidable mountain range supposedly blocks the moisture transport from the interior of the continent thus producing a rainshadow effect that is reflected in the marked east–west rainfall gradient (e.g., Houston and Hartley, 2003). Furthermore, thermally driven upslope flows force divergence along the coastal strip, depressing the top marine boundary layer and limiting the moisture flux from the Pacific Ocean into the desert during daytime (Rutllant et al., 2003).

Consistent with the nearly fixed latitudinal position of the continent during the last 150 Ma (e.g., Beck et al., 2000) and the existence of the Humboldt system since, at least, 65 Ma (Keller et al., 1997), it is generally accepted that arid/semiarid conditions ($\leq$50 mm/year) have prevailed over the Atacama region at least since the early Oligocene (Hartley, 2003; Dunai et al., 2005) and even since the late Cretaceous (Hartley et al., 2005). The onset of the current hyperarid conditions ($\leq$5 mm/year), however, is a matter of controversy as illustrated in the time-line of Fig. 2. Studies based on supergene mineralization and erosion demise in northern Chile (Alpers and Brimhall, 1988; Sillitoe and McKee, 1996) as well as pedogenesis evidence around the Calama basin (Rech et al., 2006) suggests that the Atacama underwent a marked drying between 19 and 13 Ma. Because the western flank of the Andes Cordillera raised to more than half of its actual height during the lower–middle Miocene before 10 Ma (Gregory-Wodzicki, 2000; Lamb and Hoke, 1997; Farías et al., 2005; Garzione et al., 2008), it has been proposed that such regional surface uplift was a major factor in the onset the Atacama hyperaridity by producing a rainshadow effect (e.g., Rech et al., 2006). Measurements of cosmogenic ^{21}Ne at the Atacama surfaces in the Coastal Cordillera, however, suggest an absence of significant erosion since 25 Ma (Dunai et al., 2005), thus placing the onset of hyperaridity well before the major Andean rise and eventually contributing to this uplift by the mechanism proposed by Lamb and Davis (2003).

Other studies have proposed a more recent arid-to-hyperarid transition in the Atacama. Tosdal et al. (1984), Garcia and Herail (2005), Farías et al. (2005), and Riquelme et al. (2007) observed that sedimentation on different places of the Atacama desert piedmont strongly declined by 8 Ma, signaling a marked rainfall reduction. Hartley and Chong (2002) and Hartley (2003) analyzed Neogene sediments and stratigraphy in the Preandean Central Depression of northern Chile to infer a much more recent onset of hyperaridity, between 6 and 3 Ma, and hence not being a cause nor a result of Andean uplift. Reich et al. (2009) analyzed supergene enrichment of copper deposits in the Precordillera as well as the coastal region at 23 °S suggesting an even later onset of Atacama hyperaridity ($\sim$1.5 Ma). In the later onset hypothesis, the question of what produced the transition from arid-to-hyperarid conditions in the Atacama Desert still remains, but a plausible candidate is a Pliocene cooling of the sea surface off the coast of northern Chile and southern Perú in connection with a global-scale cooling trend since the middle Miocene to present (e.g., Kennett, 1977; Zachos et al., 2001) or the end of permanent El Niño—like (warm) conditions in the tropical Pacific around 3 Ma (Federov et al., 2006; Ravelo et al., 2004).

The wide range of geological dates proposed for the onset of current hyperarid conditions in the Atacama partially arise from the different methods, scope (local versus regional conditions), record

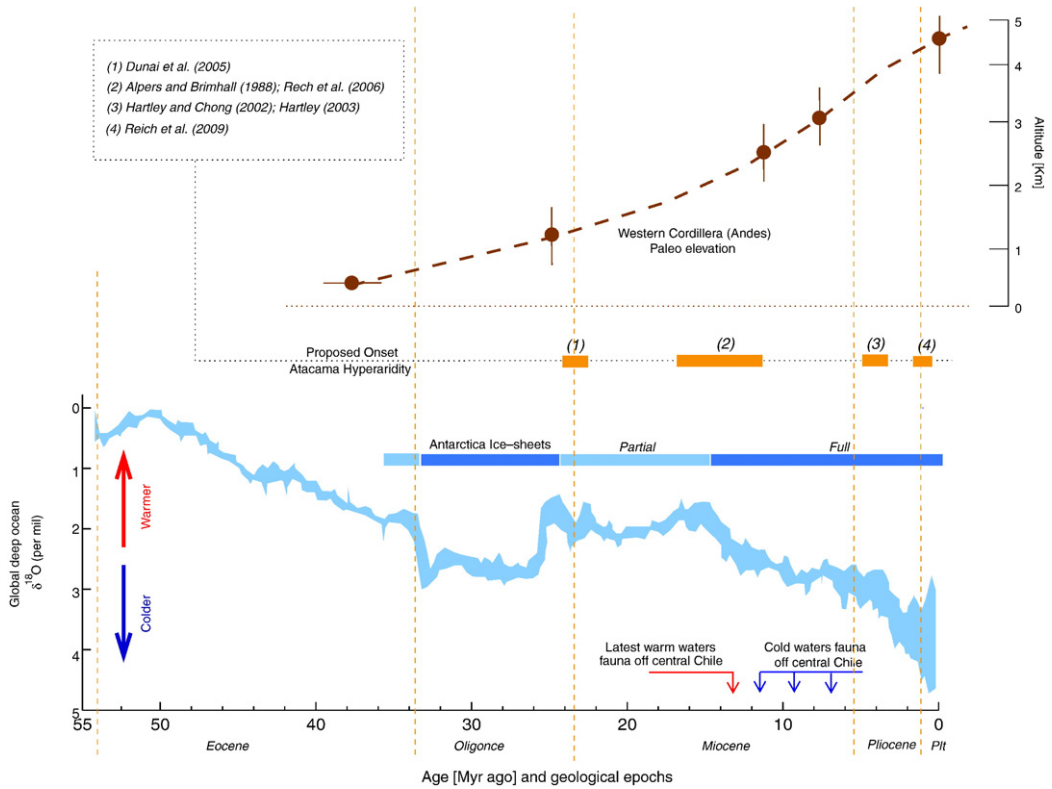

Fig. 2. Schematic chronology of the Andes cordillera paleoelevation (from Garzione et al., 2008; Farías et al., 2005; Hartley, 2003), proposed onset of Atacama hyperaridity (different sources indicated in inset), presence of Antarctic ice sheets and global deep-sea oxygen and carbonate isotopes reflecting cooling of the deep ocean and changes in ice volume (adapted from Zachos et al., 2001), and some key biotic events off north-Central Chile (from Bianucci et al., 2006; Walsh and Suárez, 2005; Ibaraki, 1992).

resolution (fine versus coarse) and location (e.g., coastal areas versus Andean foothills) of the above mentioned studies. Moreover, the geological literature is confused by an inconsistent definition of aridity, which represents the degree to which a climate lacks effective, life-promoting moisture. Long-term precipitation records allow designating a region as arid (hyperarid) when mean annual precipitation is below than 50 mm (5 mm). In contrast, paleoclimate studies can only establish the degree of aridity very indirectly upon interpretation of geological evidence. In this work, however, we have refrained of assessing the validity of the different dates proposed for the onset of Atacama hyperaridity. Likewise, inconsistencies between structural restoration and geomorphic–sedimentologic–pedogenetic data blur the Andean uplift history. In fact, propositions of late Miocene uplift are mostly sustained by sedimentological and geomorphic analysis (e.g., Garzione et al., 2008), which also could be related to climatic change raising questions on the "rapid rise model" (Ehlers and Poulsen, 2009).

The lack of a proper temporal determination of the Atacama arid-to-hyperarid transition and rise of the Andes difficult propositions about the relationships and feedbacks between both processes, in addition to the concomitant cooling of the southeast Pacific. Conceptually, both Andean uplift and southeast Pacific cooling may produce aridification of the Atacama by creating a rainshadow or increasing the atmospheric subsidence, respectively. In this contribution, we perform numerical simulations of the climate system in order to test hypotheses about the relationship between surface uplift, ocean cooling and desertification. We use the PlanetSimulator (PLASIM; Fraedrich et al., 2005a), a global climate model, to investigate more qualitatively possible interactions. We conserve the present day latitude of South America because there is evidence proposing that it has not changed much its latitudinal position since the late Cretaceous (e.g., Beck et al., 2000; Somoza and Tomlinson, 2002). Our strategy is to perform a set of model runs with one parameter altered at a time, and all the rest of the boundary conditions (earth–sun geometry, atmospheric composition and continental outlines) held constant to their present-day values. Thus, our model results are by no means "paleoclimate" simulations but they can shed light on the orography–ocean–climate relationship over western South America, by providing a first-order assessment of the relative importance of Andean uplift and ocean cooling in shaping the continental-scale climate.

2. Model setup and experiment details

The PlanetSimulator (PLASIM; Fraedrich et al., 2005a) is an Earth System Model of Intermediate Complexity (EMIC; Claussen et al., 2002) developed by the Institute of Meteorology, University of Hamburg. EMICs include all the basic component of the climate system, but some processes are simplified, thus significantly reducing the real time of their integration. PLASIM's dynamical core is a simplified Global Circulation Model (GCM) called PUMA (Fraedrich et al., 2005b) in which the moist primitive equations representing the conservation of momentum, mass and energy in the earth's atmosphere are solved numerically. PLASIM also includes a slab ocean model and zero layer model for sea ice to predict sea surface temperature (SST) and sea ice concentration, and a simple biosphere model (SIMBA) for dynamic vegetation. All our simulations were performed using a T42 version of PLASIM with 10 non-equally spaced sigma levels in the vertical (model top at 100 hPa) integrated for half a century. T42 translates to a 2.8°×2.8° latitude–longitude grid at midlatitudes, a horizontal resolution not too different from GCM-based paleoclimate and climate-change studies. This grid-spacing is also capable of resolving all the earth's major mountain ranges but with top heights about 20% less than actual values (see details in Section 3.2).

One drawback of the spectral harmonics used in PLASIM (and all spectral GCMs) is their inability to represent discontinuous features,

resulting in spurious ripples in the precipitation field near sharp topography known as the Gibbs oscillations (e.g., Navara et al., 1994). This problem is of special concern when using low horizontal resolution and considering short periods of time. In our study, the use of moderate resolution (T42) and multi-decadal climatologies minimize the Gibbs oscillations near the Andes, and no further spatial smoothing has been applied to the analyzed fields. Nevertheless, features with length scale ≤250 km near mountain ranges must be taken with caution and we rather focus in the regional-scale (length scale ≥1000 km) perspective. Whenever possible, we also compare our PLASIM outputs with results from other models with similar or higher horizontal resolution and provide a dynamical interpretation of the key modeled features.

PLASIM uses about 300 parameters prescribed to produce a simulation of the present-day climate as realistic as possible (Fraedrich et al., 2005a). These parameters include physical constants (e.g., gravity, specific heat of vaporization and Stephan-Boltzman constant), planetary values (e.g., Earth radius, Solar Constant, eccentricity and atmospheric chemical composition), and numerical values used in the representation of sub-grid processes (e.g., tuning parameter for vertical diffusion in the planetary boundary layer). An integration with these "default" parameters is referred to as Control simulation (CTL). To further increase the realism of our atmospheric simulations we turned off the slab ocean/sea ice sub-model and prescribed the lower boundary condition using the long-term monthly mean SST and Sea Ice taken from the ERSSTv2 dataset (Smith and Reynolds, 2005).

Two sets of numerical experiments were conducted: altered topography (*a*TOPO) and modified sea surface temperature (*w*SST, *u*SST and *w*SEP). In the *a*TOPO experiments the height of South American terrain was scaled by a factor $a = 0.1, 0.3, 0.5, 0.7$ and 0.9. Since the prescribed SST is identical in CTL and *a*TOPO, the differences between these two runs documents the impact of the Andes on climate due to atmospheric processes only. Three modified SST experiments were conducted using the present day (CTL) topography in each case. In the *w*SST experiment, we added 2.5 °C to the ERSSTv2 climatology in every grid point thus producing a uniform warming of the world's oceans. In the *u*SST experiment, SST was prescribed using the long-term mean zonal average (i.e., SST only varies with latitude) which effectively creates a warm anomaly along the west coast of South America mimicking a weakening of the Humboldt current and coastal upwelling. In *u*SST, however, the SST is modified over the rest of the oceans, including a cooling of the warm pool in the western tropical/subtropical Pacific. To isolate the effect of a weak Humboldt Current and coastal upwelling, we conducted the simulation *w*SEP with warming restricted to the subtropical Southeast Pacific, as describe in detail in Section 3.3.

3. Results

3.1. Control simulation

A full assessment of the PLASIM ability to simulate the present-day climate is beyond the scope of this paper. This task has been partially undertaken in recent studies using PLASIM resulting in a positive evaluation of the model performance at continental-to-planetary scales (Fraedrich et al., 2005b; Romanova et al., 2006; Kleidon et al., 2007). Nevertheless, a brief description of the CTL features over South America is necessary before analyzing the *a*TOPO and *u*SST results. Fig. 3 shows the summer (DJF) and winter (JJA) long-term mean precipitation from observations (CPC Merged Analysis of Precipitation database; Xie and Arkin, 1997) and CTL (average of last 30 years of integration). Broadly speaking, PLASIM is capable to reproduce the dominant features of the continental precipitation, including its distinctive seasonal march. During summer, a broad area of heavy precipitation encompasses central South America (10–30 °S), from the southern half of the Amazon basin to northern Argentina. The South American Monsoon is connected with the intertropical convergence zone (ITCZ) over the equatorial Atlantic and the South Atlantic convergence zone (SACZ) at subtropical latitudes. The similarity between observed and CTL summer precipitation is consistent with a realistic simulation of the northerly low-level jet over the interior of the continent (Campetella and Vera, 2002; Insel et al., 2009) shown in Fig. 4.

Over the Pacific, the observed and simulated ITCZ intersect the continent just to the north of the equator; the rest of the western coast of South America remains dry, as well as the subtropical SE Pacific, except to the south of 40 °S because of the extratropical precipitation. Of particular relevance for this study, the CTL simulation resolves the sharp gradient in precipitation between the dry west coast of subtropical South America and the wet interior. During austral winter, the tropical area of heavy precipitation migrates north of the equator producing dry conditions over Central South America, thus relaxing the east–west precipitation gradient across the subtropical Andes.

Granted, there are features in the observed fields that do not match perfectly with their model counterparts. Specifically, the CTL summer precipitation over the interior of the continent is ~1.5 times higher than observed and shifted south of its actual location, producing a precipitation deficit over central Amazonia also noted in other PLASIM-based studies (Kleidon et al., 2007). The southward displacement of the monsoonal precipitation results in a simulated Bolivian High (an upper-level anticyclone in response to the diabatic heating; e.g., Lenters and Cook, 1997), that is broader than observed as shown in Fig. 5 by the 200 hPa streamlines. This subtle error in circulation aloft is likely responsible for enhanced precipitation over the central Andes (Fig. 3) by transporting more moisture from the interior of the continent (Falvey and Garreaud, 2005), as well as a broader surface anticyclone over the SE Pacific (Fig. 5; Rodwell and Hoskins, 2001). To place these errors in context, one may consider the analysis by Vera et al. (2006) of 7 GCM simulations of the 20th century carried out for the fourth IPCC assessment report. Their Fig. 1 compares the seasonal mean precipitation amongst the models and observation, and thus it is analog to our Fig. 3; the errors in PLASIM CTL simulation are within the range of discrepancies that characterize the current generations of GCMs.

In sum, PLASIM leads to a reasonable simulated large-scale climate for present-day forcing in the context of currently available General Circulation Models, and the comparison between CTL and the sensitivity experiments does provide relevant insights. We caution the reader, however, about the moderate resolution of our results (~300 km) and a wet bias in the southern Amazon basin and Central Andes in present-day climate.

3.2. Altered topography experiments

Fig. 6 shows the summer (DJF) mean precipitation difference between the 0.3 TOPO and CTL ($\Delta P = P_{a\mathrm{TOPO}} - P_{\mathrm{CTL}}$), as well as the fractional precipitation change ($\Delta P/P_{\mathrm{CTL}}$). The factor $a = 0.3$ implies that the mean height of the Central Andes reduces from 3800 ma.s.l. in CTL (determined by the PLASIM resolution) down to ~1000 ma.s.l. in *a*TOPO, a value representative of the Andes height before its Miocene uplift (e.g., Garzione et al., 2008). The dominant feature when the topography is reduced is the weakening of the South American Monsoon: a broad area of rainfall reduction of ~5 mm/day from the southern edge of Amazonia to the subtropical plains of the continent, extending further south along the SACZ. The rainfall reduction in 0.3 TOPO, with respect to CTL, encompasses most of the Central Andes and there is a hint of reduction along the subtropical west coast of the continent, more evident when considering the fractional difference (Fig. 5b). Therefore, a reduction of the Andes height to a third of its present altitude does eliminate the rainshadow effect—by drying the subtropical plains of the continent—but does not increase the precipitation over the Atacama Desert, a key finding for the paleoclimate question posed in the introduction. The altered topography does not change significantly the advection of cold, dry air along the Atacama by

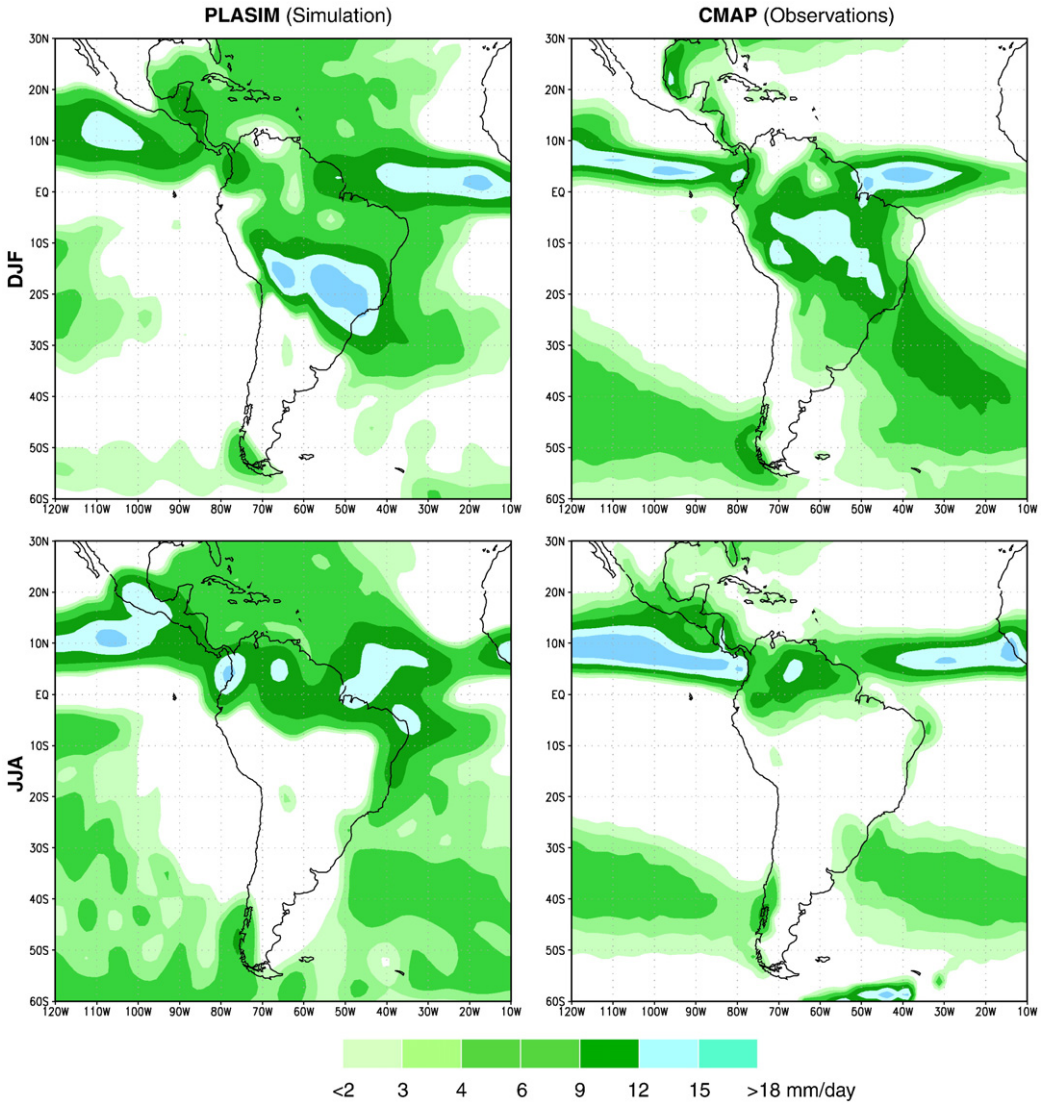

Fig. 3. Long-term mean seasonal precipitation (DJF: austral summer, JJA: austral winter) obtained from PLASIM simulations and observations. The PLASIM "climatology" is the average of the last 30 years of control simulation (see section 2). The observations are from the CPC Merged Analysis of Precipitation (CMAP) obtained by merging satellite data and ground based records from 1979 to 2005 on a 2.5°×2.5° lat–long grid (see details in Xie and Arkin, 1997).

the low-level southerly wind blowing along the coast (Fig. 4). Also noteworthy is the increase in rainfall across much of equatorial South America (including most of the Amazon Basin) and a dipole over the southern tip of the continent.

A rainfall reduction over central South America, marginally extending into the Atacama region, and rainfall increase over Amazonia when the Andes are lowered was also found by Lenters and Cook (1995) using the Geophysical Fluid Dynamics Laboratory (GFDL) GCM (see their Fig. 2), Sepulchre et al. (2009) using the French Laboratoire de Météorologie Dynamique (LDM) GCM (see their Fig. 7), and by Ehlers and Poulsen (2009) using the RegCM3 regional climate model (see their Fig. 2). The GFDL, LDM and RegCM3 models use their own set of parameterizations, numerical methods and horizontal resolutions (2.8°, 1.1° and 0.6°, respectively) lending support to our PLASIM results.

The subtropical (extratropical) precipitation differences in winter are qualitatively similar, albeit weaker (stronger) than its summer counterpart. When considering a topographic scaling factor other than 0.3, the *a*TOPO minus CTL precipitation field looks similar to the map in Fig. 6 but with varying magnitudes. Fig. 7 synthesized these results by showing the fractional precipitation change evaluated in two grid boxes to the east of the Central Andes (20 °S–65 °W) and to the west of the austral Andes (47 °S–70 °W). The rainfall reduction over central South America is slightly non-linear in contrast with the more linear behavior in the lee of the austral Andes. Note that for Central Andes heights of ~300 m ($a=0.1$) the summer rainfall over central South America reduces to about 20% of its CTL values. Fig. 7 also includes the fractional ΔP for $a=0.3$ obtained from a simulation in which both CTL and *a*TOPO were run with the slab ocean model active (i.e., calculated SST). In this case, the reduction of Andes elevation alters the atmospheric circulation and hence SST which, in turn, may alter the precipitation pattern. Nevertheless, the similarity with our previous value ($a=0.3$, prescribed SST) suggest that such an indirect effect is not discernable in our PLASIM simulations.

The topographically induced weakening of the South American Monsoon deserves further analysis as it plays a major role in the precipitation change over the Atacama region. The rainfall reduction over the central part of the continent appears directly related to a reduction in the moisture content in the lowest 3 km above the surface (not shown), from ~12 g/Kg in CTL to ~6 g/Kg in 0.3 TOPO. The later is, in turn, largely produced by the weakening of moisture transport from the Amazon Basin down to the subtropical plains, readily evident in the actual 900 hPa (about 1000 ma.s.l.) wind vectors in 0.3 TOPO and CTL (Fig. 4) as well as their difference (Fig. 5a). In present-day climate, the low-level jet (LLJ) east of the Andes owes its existence to the northern

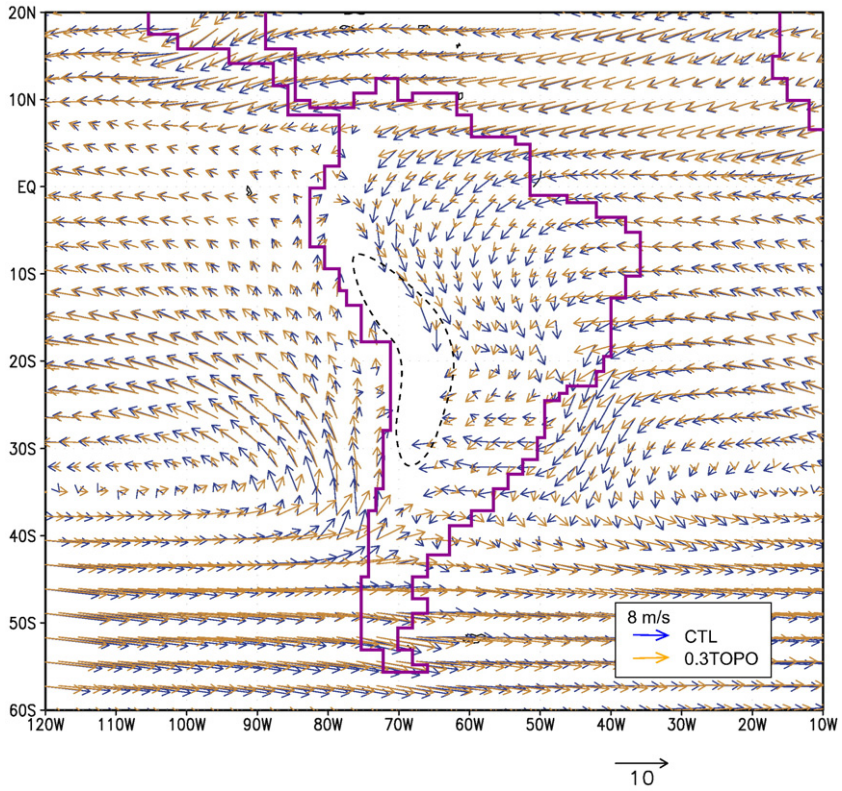

Fig. 4. Summer mean wind vectors at the 900 hPa level (about 1000 ma.s.l.) for the PLASIM's control simulation (blue arrows) and 0.3 TOPO experiment (orange arrows). In both cases the mean is calculated as the average of the last 30 years of integration. The vectors tends to coincide except over Central South America where the change in topography elevation induce a sizable reduction of the low-level northerly jet that blows parallel to the Central Andes. The dashed line indicates terrain elevation in excess of 1500 ma.s.l. in the control simulation.

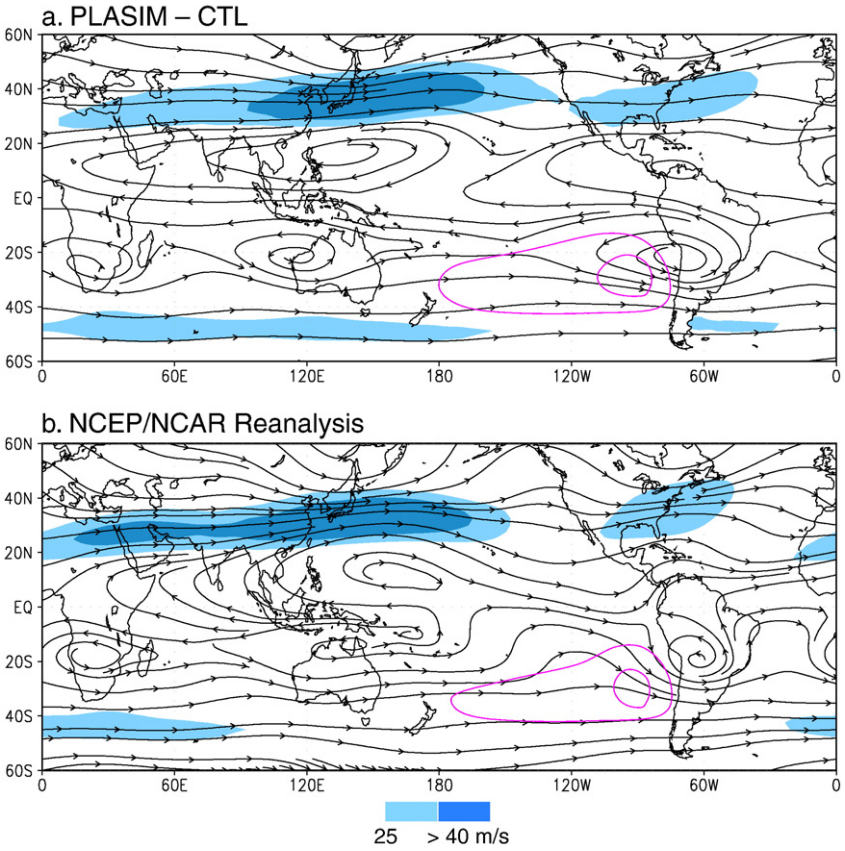

Fig. 5. Streamlines of summer (DJF) mean wind at the 200 hPa level (about 12 km ASL) in (a) PLASIM Control Simulation (CTL) and NCEP–NCAR reanalysis (observations). Also shown in light (dark) blue regions with 200 hPa wind speed above 25 (40) m/s. Magenta thin lines are the summer mean surface isobars of 1015 and 1020 hPa (innermost) over the SE Pacific signaling the subtropical anticyclone.

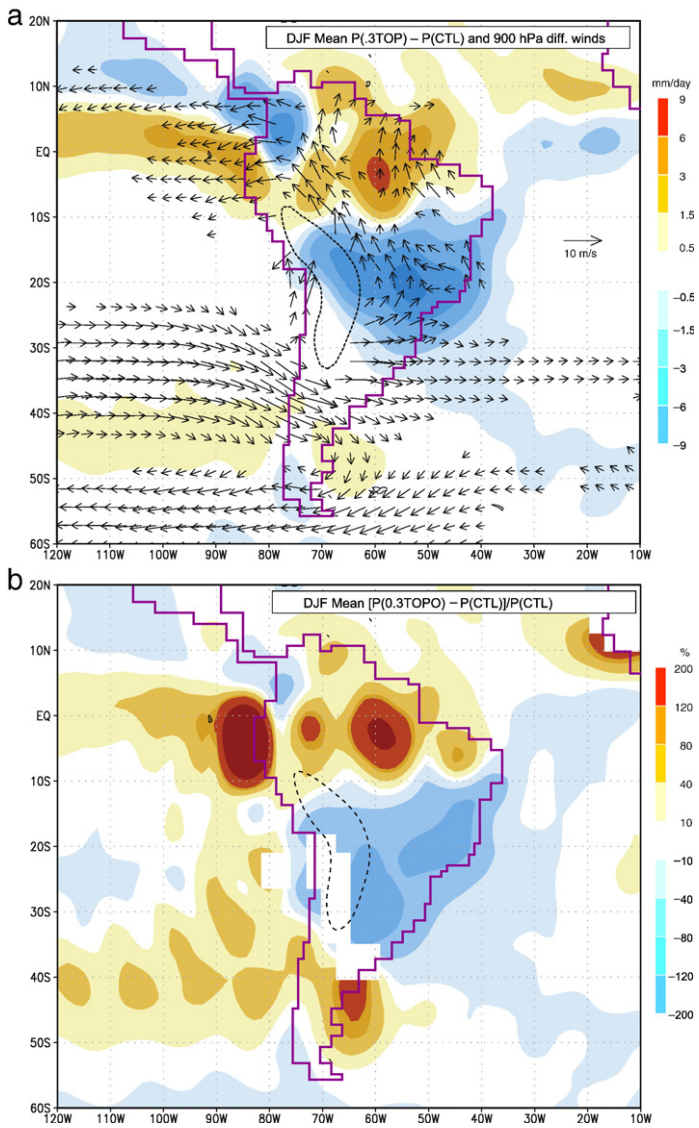

Fig. 6. (a) Summer mean precipitation difference between 0.3 TOPO experiment and the control simulation (CTL). The color scale is at right in mm/day; cold (warm) colors indicate less (more) precipitation when the topography is reduced. Also shown are the difference in 900 hPa winds between 0.3 TOPO and CTL. (b) As in (a) but for the fractional precipitation difference, that is $100\times(P_{0.3TOPO}-P_{CTL})/P_{CTL}$. The dashed line indicates terrain elevation in excess of 1500 ma.s.l. in the control simulation.

Argentina trough (Campetella and Vera, 2002; Insel et al., 2009), a low-pressure area partially maintained by the warm air that subside in the lee of the mountains. Therefore, lowering the Andes weakens the northern Argentina thermal trough and hence the LLJ, ultimately drying the interior of continent to the south of 15 °S.

3.3. Modified SST experiments

Because the coastal upwelling maintains cold surface waters along the eastern boundaries of the ocean basins, replacing the observed SST (φ,λ) (Fig. 8a) by its zonal average [SST](φ) (where φ is latitude and λ longitude) produce a warm anomaly in those regions (Fig. 8b). Off northern Chile and Perú such warming ranges from ~2.0 °C in fall to ~3.5 °C in spring, about twice larger than the regional warming during strong El Niño years in present climate (e.g., Deser and Wallace, 1990). The summer (DJF) mean precipitation difference and fractional difference between the *u*SST and CTL simulations, along with the 900 hPa wind vector difference, is shown in Fig. 9. As expected, the wind and rainfall changes are mostly confined to the ocean areas that exhibit a sizable SST difference. The east Pacific warming leads to a widespread increase in rainfall of 1.5 mm/day from the equator down to 25 °S that prevails throughout the year. The largest increases are found around 80 °W but they encompass the subtropical west of South America, also evident in the fractional precipitation change (Fig. 9b). A reduction in sea level pressure is also collocated with the region of sea surface warming (Fig. 8b,c).

A west-cooling/east-warming dipole of SST across the Pacific similar to our *u*SST boundary conditions was prescribed by Barreiero et al. (2005) to simulate the middle Pliocene climate, as it mimics a perennial El Niño conditions that presumably prevailed from 5 to 3 Ma (Ravelo et al., 2004; Wara et al., 2005). Barreiero et al. (2005) used the GFDL Atmospheric Model 2, and when comparing the Control (present day) and Pliocene (altered Pacific SST) simulations they found results similar to our *u*SST-CTL analysis. Of particular relevance, their Pliocene simulation features much more humid conditions along the subtropical band of the Southern Hemisphere (30–10 °S; their Fig. 5) and significant precipitation along the subtropical west coast of South America (their Fig. 7), both consistent with a reduction of Atacama aridity.

In the *w*SST experiment we replaced the observed climatology by $SST(\varphi,\lambda)+2.5$ °C everywhere. In this globally warmer experiment the changes in precipitation off and along the northern Chile–southern

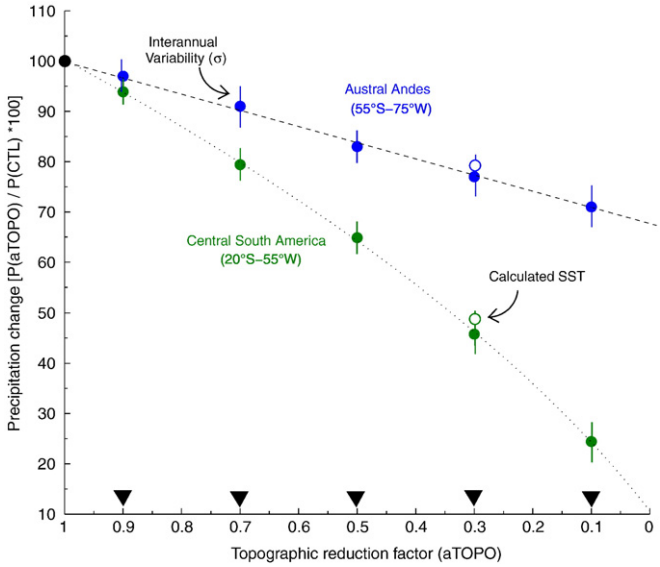

Fig. 7. Fractional precipitation reduction, that is $100 \times P_{aTOPO}/P_{CTL}$ for each *a*TOPO experiments ($a = 0.9, 0.7, 0.5, 0.3, 0.1$; triangles at bottom) evaluated in two grid boxes. The blue solid symbols are for a box centered at 55 °S/75 °W just upstream of the Austral Andes. The green solid symbols are for a box centered at 20 °S/55 °W over the Bolivian lowlands (east of the Central Andes). The vertical bars indicate the interannual variability considering the last 30-year of each experiment, which is rather small since PLASIM was forced with a prescribed, constant seasonal cycle of SST and Sea Ice. For $a = 0.3$ the open circles indicate the fractional precipitation reduction when PLASIM was integrated with the active ocean model (calculated SST).

Perú coast are less than 0.2 mm/day (not shown), emphasizing the crucial role of the regional warming to produce a significant reduction in Atacama's aridity. In other words, the key ingredient of Atacama's aridity is not the adjacent cold ocean per se, but rather the meridional gradient of SST between the eastern and central subtropical Pacific.

We diagnosed the precipitation change over the subtropical SE Pacific using a simplified water vapor budget following Lenters and Cook (1995). In essence, the climatological precipitation field P is decomposed as the sum of several terms related to features of the large-scale circulation (vertically integrated mean convergence and advection of moisture, evaporation, orographically forced ascent, and transient terms). It turns out that the increased precipitation in *u*SST is mainly due to enhanced moisture convergence moisture transport (50% of the difference), and evaporation (28%). In *w*SST the modest increase in precipitation is only due to enhanced evaporation. We can further interpret these terms as actual thermodynamic and dynamical processes. Warmer SSTs moisten and deepen the atmospheric boundary layer locally, conducive to the formation of trade wind cumuli in replacement of the stratus deck observed in the present climate. Trade wind cumuli often produce light rain in contrast with the non-precipitating stratus clouds. From a dynamical perspective, the regional warming in *u*SST weakens the subsidence as signaled by the cyclonic circulation anomaly at 900 hPa (Fig. 9a) and sea level pressure anomalies of about 2 hPa over the SE Pacific. Ultimately, a weaker subtropical anticyclone reduces the advection of cool, dry air at low levels off northern Chile and southern Perú, and allows more frequent passage mid-latitude disturbances the north of 30 °S.

The altered circulation and precipitation in *u*SST with respect to CTL may arise not only because the warming of the subtropical southeast Pacific but also from changes in SST elsewhere, particularly the cooling of the western tropical Pacific (Fig. 8b). To isolate the effect of the sea surface warming near the west coast of South America, we carried out a third experiment in which SST was only altered over the Southeast Pacific (*w*SEP) as shown in Fig. 8c. East of 100 °W the precipitation differences *w*SEP-CTL are almost identical to the *u*SST-CTL counterpart (not shown), indicating that most of the precipitation along the west coast of subtropical South America arises from the local effect of the warming rather than remote influences.

4. Discussion

While the two set of experiments conducted with PLASIM are not paleoclimate simulations (because most of the boundary conditions were set to present-day climates) we can use our results to construct a "what-if" story of the Atacama's climate. The altered topography (*a*TOPO) experiments are relatively simply to put on a time-line (but with significant uncertainty in the exact timing) as the modern uplift of the Central Andes, and particularly its western flank, is a monotonic processes that began at least 25 Ma ago and there is some confidence in that the Andes reached more than half of its elevation by 8 Ma ago (Lamb and Hoke, 1997; Gregory-Wodzicki, 2000; Farías et al., 2005; Garzione et al., 2008). Our results suggest that the Andean surface uplift had little, if any, effect on the lack of precipitation and moisture over the Atacama, regardless of the age of uplift (which is still matter of debate). The SE Pacific and the adjacent west coast of South America remains under strong tropospheric subsidence and cool air advection from southerly winds (hindering precipitation) regardless of the Andes height. Accordingly, the Andean uplift does not appear as an important ingredient in the onset of Atacama hyperaridity, even if both events overlapped in time.

Nevertheless, the gradual uplift of the Andes during most of the late Cenozoic appears as a key factor in extending the area of convective precipitation over the interior of the continent from low-latitudes (Amazon Basin) into the subtropics along and to the east of the Central Andes, as to create the present-day South American Monsoon and "Bolivian winter". This modeling result is consistent with geological evidence on the eastern side of the Andes that suggest an onset of humid climate conditions in late Miocene time (Strecker et al., 2007 and references therein). However, our modeling did not considered possible marine transgressions over Amazonia, southern Bolivia and northern Argentina in the Miocene (e.g., Hernandez et al., 2005) which, acting as a moisture source, may have altered the continental climate. One also must keep in mind that the progressive wet conditions over today's Bolivia, southern Brazil and northern Argentina instigated by the Andean uplift and low basins emersion may have partially offset by the planetary scale cooling during most of the Neogene (e.g., Zachos et al., 2001).

The key finding of our *u*SST and *w*SEP experiments is that a regional warm anomaly of a few degrees over the SE Pacific results in a

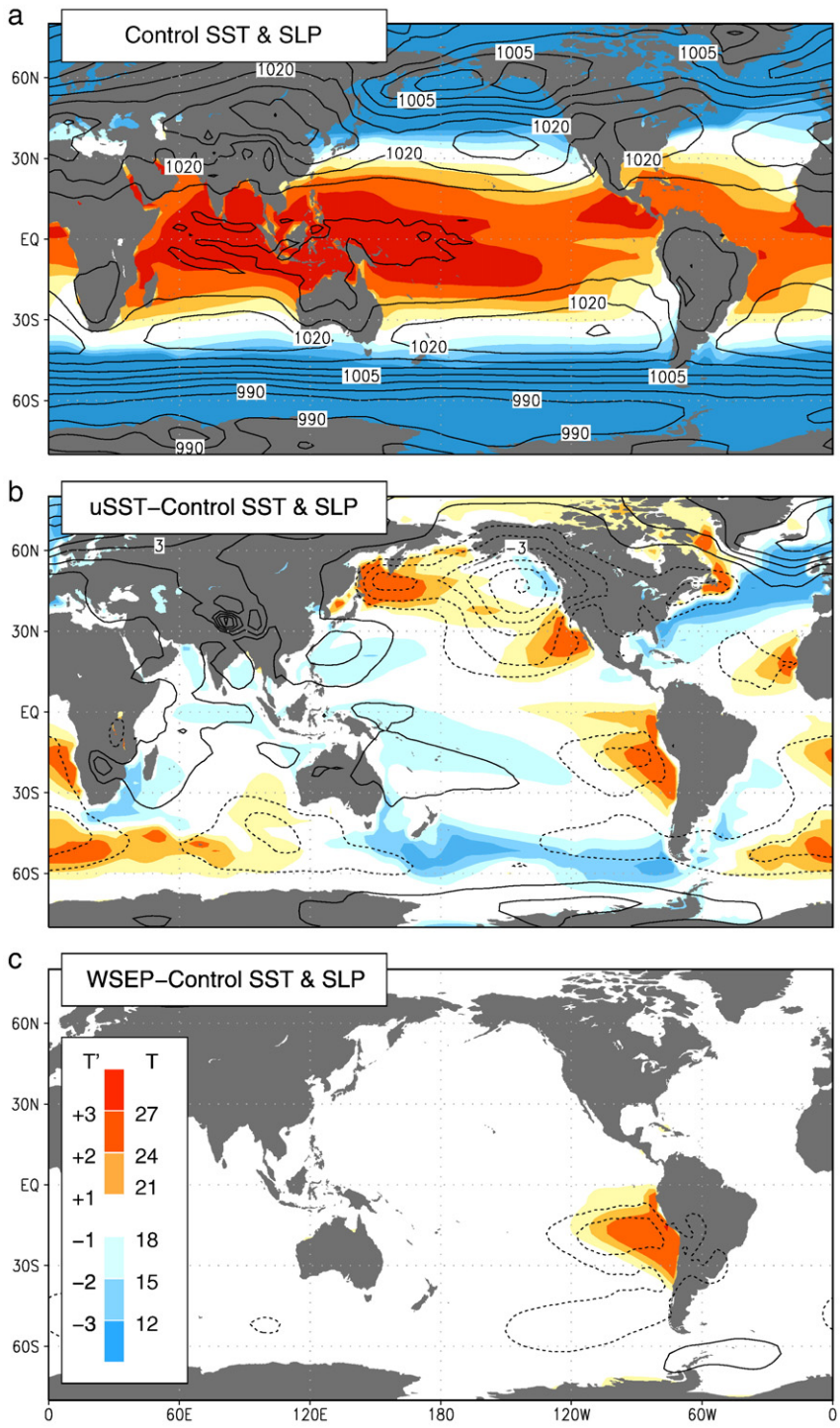

Fig. 8. Annual mean sea surface temperature (SST, colors in °C according to the right scale in panel c) and sea level pressure (SLP, contoured every 2.5 hPa). The SST field is prescribed (no calculated by the model) in our PLASIM simulations. (b) SST anomalies (colors in °C according to the left scale in panel c) superimposed on the mean field as to produce a zonally uniform SST field (prescribed in our *u*SST simulation). Contours are the annual mean SLP anomalies (every 1 hPa) produced by PLASIM in *u*SST. (c) SST anomalies (colors in °C according to the left scale in panel c) superimposed in the mean field as to produce a warming of the subtropical Southeast Pacific (prescribed in our *w*SEP simulation). Contours are the annual mean SLP anomalies (every 1 hPa) produced by PLASIM in *w*SEP.

significant increase in moisture and precipitation over the west coast of subtropical South America. This result, however, is less simple to put on a time-line. Although worldwide records of deep-sea oxygen and carbon (e.g., Zachos et al., 2001) do reveal a cooling trend from the Middle Miocene to the present (Fig. 2) the relevant question is when, if ever, a weakened Humboldt system condition (i.e., regional warming) took place. The Humboldt system, involving both coastal upwelling and advection of cold waters from higher latitudes, has been active at least since the lower Cenozoic (Keller et al., 1997). Nevertheless, presence of tropical/subtropical faunas dating back to 15 Ma has been documented off central Chile (Bianucci et al., 2006; Walsh and Suárez, 2005) indicative of a weakened Humboldt system prior to that date. Its subsequent reinforcement during the middle Miocene, signaled by the appearance of cold-adapted planktonic foraminifera off Chile (Ibaraki, 1992), has been attributed to the strengthening of the equatorward advection of cold subpolar waters

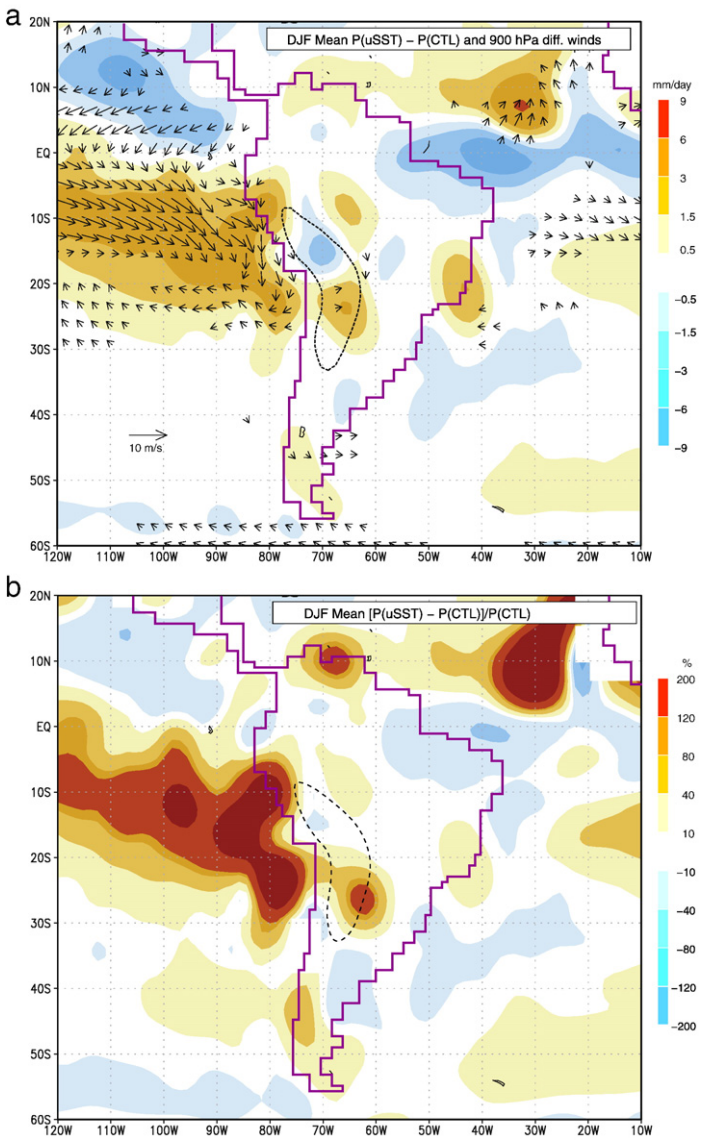

Fig. 9. (a) Summer mean precipitation difference between *u*SST experiment and the control simulation (CTL). The color scale is at right in mm/day; cold (warm) colors indicate a less (more) precipitation when the SST is prescribed as function of latitude only. Also shown are the difference in 900 hPa winds between *u*SST and CTL. (b) As in (a) but for the fractional precipitation difference, that is $100\times(P_{uSST}-P_{CTL})/P_{CTL}$. The dashed line indicates terrain elevation in excess of 1500 ma.s.l. in the control simulation.

into the south Humboldt system (e.g., Mohtadi et al., 2005) in connection with the onset of glaciation of Antarctica. The impact of sea surface temperature anomalies at midlatitudes in the SH upon the tropical Pacific due to changes in the subtropical gyre (including the Humboldt system) has also demonstrated in coupled ocean–atmosphere model experiments by Lee and Poulsen (2005).

A further cooling of the tropical–subtropical east Pacific likely took place during the Pliocene/Pleistocene transition (Cannariato and Ravelo, 1997; Ravelo et al., 2004; Haywood et al., 2005) following the closing of the Panama seaway around 4.3 Ma (e.g., Haug et al., 2001). Foraminifera Mg/Ca ratio also suggests that the present-day east–west SST gradient across the tropical/subtropical Pacific began 3 Ma (Wara et al., 2005) since the ocean basin was locked in permanent El Niño-like state during the Pliocene (Federov et al., 2006; Barreiero et al., 2005). If this interpretation is correct, our *w*SEP and *u*SST would represent a first approximation of the middle Pliocene climate (as in Barreiero et al., 2005) placing the arid-to-hyperarid transition in the Atacama after 3 Ma. This timing lends support to the later onset of Atacama hyperaridity proposed by geological evidence (e.g., Hartley and Chong, 2002; Farías et al., 2005; Reich et al., 2009).

In closing this section, we note that the effect of mountain height and SST on maintaining the Atacama's hyperaridity derived from our PLASIM may be generally applicable to other landmasses. Each of the Earth's subtropical deserts is bounded to the west by relatively cold oceans, with coastal SST 2–3 °C lower than the zonal average. The geomorphologic features inland, however, are quite different and only the Atacama Desert is bounded to the west by a very high, continuous mountain range. The presence of a mountain range may be more relevant determining the warm season continental precipitation to its west, by channeling the moisture from the tropics into subtropical latitudes. Fig. 10 encapsulate this global perspective by showing the relationship between precipitation, SST and mountain height for selected subtropical sites.

5. Conclusions

Gentle but persistent descent of air in the subtropical margin of the Hadley cell is the first-order climatic control of the world largest desert. The evidence of long-lived dry condition along the western border of subtropical South America is therefore consistent with nearly fixed

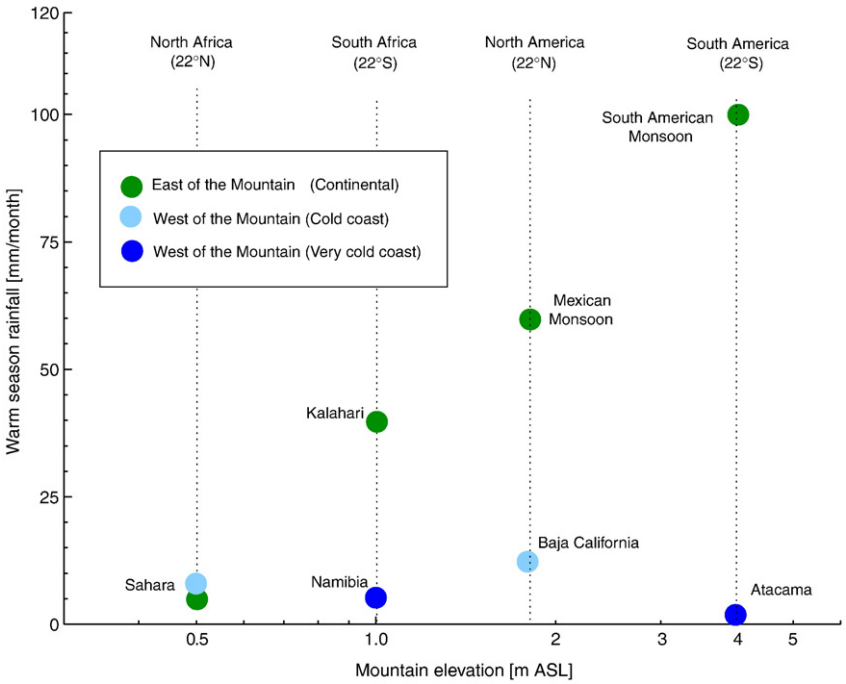

Fig. 10. General relationship among mountain elevation and observed sea surface temperature (ERSST) and precipitation (CMAP) at subtropical latitudes (21–23 °N and 21–23 °S). For each of the geographical areas indicated atop we identified the axis of maximum terrain elevation (mountain or plateau ridge) calculated the average mountain height and the warm season precipitation immediately to west (green circles) and east (blue circles) of the ridge. The precipitation is plotted as a function of the mountain elevation. The precipitation to the east of the mountains, representing coastal subtropical deserts, is color coded according to the SST off the coast: dark (light) blue represent very cold (moderately cold) conditions. Note that continental warm season precipitation is strongly dependent of the mountain height, while coastal precipitation is essentially unrelated to it.

latitudinal position of this continent since the late Cretaceous. Furthermore, mounting geological evidences of different nature (supergene mineralization and erosion demise, pedogenesis, stratigraphy and cosmogenic ^{21}Ne) obtained in the core of the Atacama Desert indicate a transition from arid (average annual rainfall ≤50 mm) to hyperarid (average annual rainfall ≤5 mm) during the Neogene. The timing of this transition is, however, weakly constrained ranging from 25 Ma to 1.5 Ma, hindering its attribution to the concomitant rise of the central Andes western flank (e.g., Garzione et al., 2008), global cooling (e.g., Zachos et al., 2001) and emergence of cold waters off the west coast of South America (e.g., Cannariato and Ravelo, 1997). In this paper, we have studied potential links among these major geological, atmospheric and oceanographic events by performing numerical experiments using PLASIM, an earth model of intermediate complexity.

The key finding of our altered SST experiments is that a regional warm anomaly of a few degrees over the SE Pacific results in a reduction of the subsidence and anticyclonic flow as well as a significant increase in moisture and precipitation along the west coast of subtropical South America. Thus, our simulation and available paleoevidence suggest that sea surface cooling off Chile/Perú since the late Miocene and, especially, during the Pliocene/Pleistocene transition, very effectively resulted in a drying over the Atacama Desert, either gradual or stepwise, that culminated with the present day hyperarid conditions. In contrast, the dry conditions, tropospheric subsidence and low-level anticyclonic flow along the west coast of South America experience little change in the experiments when the Andean elevation is reduced by factor 0.9 to 0.1. These result from PLASIM are consistent with other climate simulations performed with independent models (e.g., Ehler and Poulsen, 2009; Sepulchre et al., 2009). Thus, our results suggest that the Andean surface uplift had little, if any, effect on the lack of precipitation and moisture over the Atacama, regardless of the age of uplift (which is still matter of debate).

We stressed that our modeling results are not paleoclimate simulations, as they only varied one setting (SST or topography) at a time, keeping constant other parameters. Simulations with conditions fully representing key temporal slices during the Neogene are currently underway, particularly at times of maritime transgression that may had substantially altered the continental climate.

Acknowledgements

This work was supported by CONIYCT-Chile grants ACT-19, ACT-18, R9, R7 and FONDECYT 11085022. We thank Dr. Jose Cembrano and one anonymous reviewer for excellent constructive criticism of the original manuscript.

References

Alpers, C., Brimhall, G., 1988. Middle Miocene climatic change in the Atacama Desert, northern Chile: Evidence from supergene mineralization at La Escondida. Bulletin of the Geological Society of America 100 (10), 1640.

Barreiero, M., Philander, S., Pacanowski, R.C., Federov, A.V., 2005. Simulations of warm tropical conditions with application to middle Pliocene atmospheres. Clim. Dyn. doi:10.1007/s00382-005-0086-4.

Beck, M., Burmester, R., Cembrano, J., Drake, R., García, A., Hervé, F., Munizaga, F., 2000. Paleomagnetism of the North Patagonian Batholith, southern Chile. An exercise in shape analysis. Tectonophysics 326 (1–2), 185–202.

Bianucci, G., Sorbi, S., Suárez, M., Landini, W., 2006. The southernmost sirenian record in the eastern Pacific Ocean, from the Late Miocene of Chile. Comptes Rendus Palevol 5, 945–952.

Campetella, C., Vera, C., 2002. The influence of the Andes mountains on the South American low-level flow. Geophys. Res. Lett. 29, 1826.

Cannariato, K., Ravelo, A., 1997. Pliocene–Pleistocene evolution of eastern tropical Pacific surface water circulation and thermocline depth. Paleoceanography 12, 805–820.

Claussen, M., et al., 2002. Earth system models of intermediate complexity: closing the gap in the spectrum of climate system models. Clim. Dyn. 18, 579–586.

Deser, C., Wallace, J., 1990. Large-scale atmospheric circulation features of warm and cold episodes in the tropical Pacific. J. Climate 3, 1254–1281.

Dunai, T., González López, G., Juez-Larré, J., 2005. Oligocene–Miocene age of aridity in the Atacama Desert revealed by exposure dating of erosion-sensitive landforms. Geology 33, 321–324.

Ehlers, T., Poulsen, C., 2009. Influence of Andean uplift on climate and paleoaltimetry estimates. Earth Planet. Sci. Lett. 281, 238–248.

Falvey, M., Garreaud, R., 2005. Moisture variability over the South American Altiplano during the SALLJEX observing season. J. Geophys. Res. 110, D22105. doi:10.1029/2005JD006152.

Farías, M., Charrier, R., Comte, D., Martinod, J., Hérail, G., 2005. Late Cenozoic deformation and uplift of the western flank of the Altiplano: evidence from the depositional, tectonic, and geomorphologic evolution and shallow seismic activity (northern Chile at 19°30'S). Tectonics 24, TC4001.
Federov, A.V., Dekens, P.S., McCarthy, M., Ravelo, A.C., deMenocal, P.B., Barreiero, M., Pacanowski, R.C., Philander, S., 2006. The Pliocen paradox (Mechanism for a permanent El Niño). Science 312, 1485–1489.
Fraedrich, K., Jansen, H., Kirk, E., Luksch, U., Lunkeit, F., 2005a. The planet simulator: towards a user friendly model. Meteorol. Z. 14, 299–304.
Fraedrich, K., Jansen, H., Kirk, E., Lunkeit, F., 2005b. The planet simulator: green planet and desert world. Meteorol. Z. 14, 305–314.
Garcia, M., Herail, G., 2005. Fault-related folding, drainage network evolution and valley incision during the Neogene in the Andean Precordillera of Northern Chile. Geomorphology 65, 279–300.
Garreaud, R., Rutllant, J., 1996. Análisis meteorológico de los aluviones de Antofagasta y Santiago de Chile en el periodo 1991–1993. Atmósfera. 9, 251–271.
Garreaud, R., Vuille, M., Clement, A., 2003. The climate of the Altiplano: observed current conditions and mechanisms of past changes. Palaeogeogr. Palaeoclimatol. Palaeoecol. 194, 5–22.
Garzione, C., et al., 2008. Rise of the Andes. Science 320, 1304–1307.
Gregory-Wodzicki, K.M., 2000. Uplift history of the Central and Northern Andes: a review. Bull. Geol. Soc. Am. 112, 1091–1105.
Hartley, A., 2003. Andean uplift and climate change. J. Geol. Soc. 160, 7–10.
Hartley, A., Chong, G., 2002. Late Pliocene age for the Atacama Desert: implications for the desertification of western South America. Geology 30, 43–46.
Hartley, A.J., Chong, G., Houston, J., Mather, A.E., 2005. 150 million years of climate stability: Evidence from the Atacama Desert, northern Chile. Geological Society of London Journal 162, 421–441.
Haug, G., Tiedemann, R., Zahn, R., Ravelo, A., 2001. Role of Panama uplift on oceanic freshwater balance. Geology 29, 207–210.
Haywood, A.M., Dekens, P., Ravelo, A.C., Williams, M., 2005. Warmer tropics during the mid-Pliocene? Evidence from alkenone paleothermometry and a fully-coupled ocean–atmosphere GCM. Geochem. Geophys. Geosys. 6. doi:10.1029/2004GC000799.
Hernandez, R.M., Jordan, T.E., Dalenz Farjat, A., Echavarría, L., Idleman, B.D., Reynolds, J.H., 2005. Age, distribution, tectonics, and eustatic control of the Paranense and Caribbean marine transgressions in Southern Bolivia and Argentina. J. S. Am. Earth Sci. 19, 495–512.
Houston, J., Hartley, A., 2003. The Central Andean west-slope rainshadow and its potential contribution to the origin of hyper-aridity in the Atacama Desert. Int. J. Climatol. 23, 1453–1464.
Ibaraki, M., 1992. Planktonic foraminifera from the Navidad Formation, Chile: their geologic age and paleoceanographic implications. Centenary of Japanese Micropaleontology. Terra Scientific, Tokyo, pp. 91–95.
Insel, N., Poulsen, C.J., Ehlers, T.A., 2009. Influence of the Andes Mountains on South America moisture, transport, convection and precipitation. Clim. Dyn. doi:10.1007/s00382-009-0637-1.
Keller, G., Adatte, T., Stinnesbeck, W., Stüben, D., Kramar, U., Berner, Z., Li, L., Perch-Nielsen, K., 1997. The Cretaceous-Tertiary transition on the shallow Saharan Platform of southern Tunisia. Geobios 30 (7), 951–975.
Kennett, J., 1977. Cenozoic evolution of Antarctic glaciation, the circum-Antarctic Ocean, and their impact on global paleoceanography. J. Geophys. Res. Oceans 82.
Kleidon, A., Fraederich, K., Low, C., 2007. Multiple steady-state in the terrestrial atmosphere–biosphere system. Biogeosciences 4, 707–714.
Lamb, S., Davis, P., 2003. Cenozoic climate change as a possible cause for the rise of the Andes. Nature 425, 792–797.
Lamb, S., Hoke, L., 1997. Origin of the high plateau in the Central Andes, Bolivia, South America. Tectonics 16.
Lenters, J., Cook, K., 1995. Simulation and diagnosis of the regional summertime precipitation climatology of South America. J. Climate 8, 2988–3005.
Lenters, J., Cook, K., 1997. On the origin of the Bolivian high and related circulation features of the South American climate. Journal of the Atmospheric Sciences 54 (5), 656–678.
Lee, S., Poulsen, C., 2005. Tropical Pacific climate response to obliquity forcing in the Pleistocene. Paleoceanography 20 (4).
Lettau, H., 1978. Explaining the World's Driest Climate. Univ. of Wis. Pres, Madison.
Mohtadi, M., Hebbeln, D., Marchant, M., 2005. Upwelling and productivity along the Peru–Chile Current derived from faunal and isotopic compositions of planktic foraminifera in surface sediments. Mar. Geol. 216, 107–126.
Navara, A., Stern, W., Miyakoda, K., 1994. Reduction of the Gibbs oscillation in spectral model simulations. J. Climate 7, 1169–1183.
Peterson, T., Vose, R., 1997. An overview of the Global Historical Climatology Network temperature database. Bull. Am. Meteorol. Soc. 78, 2837–2849.
Ravelo, A., Andreasen, D., Lyle, M., Lyle, A., Wara, M., 2004. Regional climate shifts caused by gradual global cooling in the Pliocene epoch. Nature 429, 263–267.
Rech, J., Currie, B., Michalski, G., Cowan, A., 2006. Neogene climate change and uplift in the Atacama Desert, Chile. Geology 34, 761–764.
Reich, M., et al., 2009. Supergene enrichment of copper deposits since the onset of modern hyperaridity in the Atacama Desert, Chile. Miner. Deposita 1432–1866.
Riquelme, R., Hérail, G., Martinod, J., Charrier, R., Darrozes, J., 2007. Late Cenozoic geomorphologic signal of Andean forearc deformation and tilting associated with the uplift and climate changes of the Southern Atacama Desert (26°S–28°S). Geomorphology 86 (3–4), 283–306.
Rodwell, M., Hoskins, B., 2001. Subtropical anticyclones and summer monsoons. J. Climate 14 (15), 3192–3211.
Romanova, V., Lohmann, G., Grosfeld, K., 2006. Effect of land albedo, CO_2, orography and oceanic heat transport on extreme climates. Clim. Past 2, 31–42.
Rutllant, J., Fuenzalida, H., Aceituno, P., 2003. Climate dynamics along the arid northern coast of Chile: the 1997–1998 Dinámica del Clima de la Región de Antofagasta (DICLIMA) experiment. J. Geophys. Res. 108, 4538.
Sepulchre, P., Sloan, L., Fluteau, F., 2009. Modeling the response of Amazonian climate to the uplift of the Andes. In: Hoorn, C., Vonhof, H. (Eds.), Amazonia, Landscapes and Species Evolution.
Sillitoe, R., McKee, E., 1996. Age of supergene oxidation and enrichment in the Chilean porphyry copper province. Economic Geology 91 (1), 164.
Smith, T., Reynolds, R., 2005. A global merged land–air–sea surface temperature reconstruction based on historical observations. J. Climate 18, 2021–2036.
Somoza, R., Tomlinson, A., 2002. Paleomagnetism in the Precordillera of northern Chile (22°30′S): implications for the history of tectonic rotations in the Central Andes. Earth Planet. Sci. Lett. 194, 369–381.
Strecker, M., et al., 2007. Tectonics and climate of the Southern Central Andes. Annu. Rev. Earth Planet. Sci. 35, 747–787.
Takahashi, K., Battisti, D., 2007. Processes controlling the mean tropical Pacific precipitation pattern. J. Climate 20, 3434–3451.
Tosdal, R.M., Clark, A.H., Farrar, E., 1984. Cenozoic polyphase landscape and tectonic evolution of the Cordillera Occidental, southern Peru. Geol. Soc. Am. Bull. 95, 1318–1332.
Vargas, G., Rutllant, J., Ortlieb, L., 2006. ENSO climate teleconnections and mechanisms for Holocene debris flows along the hyperarid coast of western South America (17–24 S). Earth Planet. Sci. Lett. 249, 467–483.
Vera, C., et al., 2006. Toward a unified view of the American Monsoon Systems. J. Climate 19, 4977–5000.
Virji, H., 1981. A preliminary study of summertime tropospheric circulation patterns over South America estimated from cloud winds. Monthly Weather Review 109 (3), 599–610.
Vuille, M., Bradley, R., Keimig, F., 2003. Interannual climate variability in the Central Andes and its relation to tropical Pacific and Atlantic forcing. J. Geophys. Res. Atmos. 105.
Walsh, S., Suárez, M., 2005. First post-Mesozoic record of Crocodyliformes from Chile. Acta Palaeontol. Pol. 50, 595.
Wang, Y., Xie, S., Xu, H., Wang, B., 2004. Regional model simulations of marine boundary layer clouds over the Southeast Pacific off South America. Part I: Control experiment. Mon. Weather Rev. 132, 274–296.
Wara, M., Ravelo, A.C., Delaney, M.L., 2005. Permanent El Niño conditions during the Pliocene warm period. Science 309, 758–761.
Xie, P., Arkin, P., 1997. Global precipitation: a 17-year monthly analysis based on gauge observations, satellite estimates, and numerical model outputs. Bull. Am. Meteorol. Soc. 78, 2539–2558.
Zachos, J., Pagani, M., Sloan, L., Thomas, E., Billups, K., 2001. Trends, rhythms, and aberrations in global climate 65 Ma to present. Science 292, 686–693.
Zhou, J., Lau, K., 1998. Does a monsoon climate exist over South America? J. Climate 11, 1020–1040.

Further reading

Beck, M.E., 1999. Jurassic and Cretaceous apparent polar wander relative to South America: some tectonic implications. J. Geophys. Res. 104, 5063–5068.
Rasanen, M., Linna, A., Santos, J., Negri, F., 1995. Late Miocene tidal deposits in the Amazonian foreland basin. Science 269 (5222), 386–390.